Evaluation of Sentinel-2 time-series for mapping floodplain grassland plant communities

Sebastien Rapinel, Cendrine Mony, Lucie Lecoq, Bernard Clement, Alban Thomas, Laurence Hubert-Moy

Remote Sensing of Environment 223 (2019) 115–129

Contents lists available at ScienceDirect

Remote Sensing of Environment

journal homepage: www.elsevier.com/locate/rse

Evaluation of Sentinel-2 time-series for mapping floodplain grassland plant communities

Sébastien Rapinel[a,*], Cendrine Mony[b], Lucie Lecoq[b], Bernard Clément[b], Alban Thomas[a], Laurence Hubert-Moy[a]

[a] CNRS UMR 6554 LETG, University of Rennes 1, Place du Recteur Henri Le Moal, 35000 Rennes, France
[b] CNRS UMR 6553 ECOBIO, University of Rennes 2, Avenue Général Leclerc, 35000 Rennes, France

ARTICLE INFO

Keywords:
Vegetation
Wetlands
Natural habitats
Phytosociology
EUNIS

ABSTRACT

Monitoring grassland plant communities is crucial for understanding and managing biodiversity. Previous studies indicate that mapping these natural habitats from single-date remotely sensed imagery remains challenging because some communities have similar physiognomy. The recently launched Sentinel-2 satellites are a promising opportunity for monitoring vegetation. This article assesses the advantages of Sentinel-2 time-series for discriminating plant communities in wet grasslands. An annual Sentinel-2 time-series was compared respectively to single-date and single-band datasets derived from this time-series for mapping grassland plant communities in a temperate floodplain located near Mont-Saint-Michel Bay, which is included in the long-term ecological research network "ZA Armorique" (France). At this 475 ha site, 123 vegetation relevés were collected and assigned to seven plant communities to calibrate and validate the Sentinel-2 data. Satellite images were classified using support vector machine (SVM) and random forest (RF) classifiers. Results show that the SVM classifier performs slightly better than the RF classifier (overall accuracy 0.78 and 0.71, respectively). They highlight that accuracy is lower when using single-date (0.67) or single-band images (0.70). The results also reveal that discrimination of plant communities is more sensitive to temporal resolution ($\Delta = 0.34$ in overall accuracy) than spectral resolution ($\Delta = 0.12$ in overall accuracy).

1. Introduction

Plant communities, defined as frequently co-occurring plant species (Biondi, 2011), are considered the fundamental unit of natural habitats (Rodwell et al., 2018). Monitoring plant communities is crucial for managing biodiversity. Plant communities, which are a static and visible expression of biotic and abiotic dynamics, are commonly considered relevant indicators of ecosystem health (Maltby and Barker, 2009). More precisely, plant communities are suitable for mapping ecosystem services (Lavorel et al., 2011) or assessing the conservation status of a site (Berg et al., 2014), especially in wetlands, which perform many hydrological, biogeochemical and ecological functions and services (Maltby and Acreman, 2011). Plant communities can have short-term (i.e. annual) spatio-temporal dynamics related to hydrological management and agricultural practices (Dumont et al., 2012). Consequently, regular monitoring of plant communities is required to assess impacts of conservation plans on floristic biodiversity. Time-consuming field-based approaches - using aerial photographs as a basis for mapping - are still the most common methods used to map plant communities (Zlinszky et al., 2014), make annual updates infeasible for areas larger than a few hundred hectares and raise obvious issues about mapping consistency (Ullerud et al., 2018), while remote sensing data remain underused by environmental managers (Vanden Borre et al., 2011).

Over the past decade, very high spatial resolution remote sensing data were assessed for mapping wetland vegetation (Guo et al., 2017). Many studies have highlighted that plant formations (i.e. vegetation units with similar physiognomy such as woods, shrubs, fens, and grasslands) can be mapped with high accuracy (Kappa index > 0.8) using single-date multispectral imagery (Rapinel et al., 2014) or LiDAR data (Chasmer et al., 2014). Nevertheless, plant formations often encompass many plant communities that are distributed according to environmental variables such as soil moisture (Marion et al., 2010) or grazing intensity (Dumont et al., 2012). Consequently, mapping plant formations is inappropriate for monitoring natural habitats because many plant communities are merged into the same vegetation unit. Conversely, multispectral single-date data have been shown unsuitable for accurately mapping plant communities; for example, Martínez-

* Corresponding author.
E-mail address: sebastien.rapinel@univ-rennes2.fr (S. Rapinel).

https://doi.org/10.1016/j.rse.2019.01.018
Received 16 October 2017; Received in revised form 17 September 2018; Accepted 13 January 2019
Available online 21 January 2019

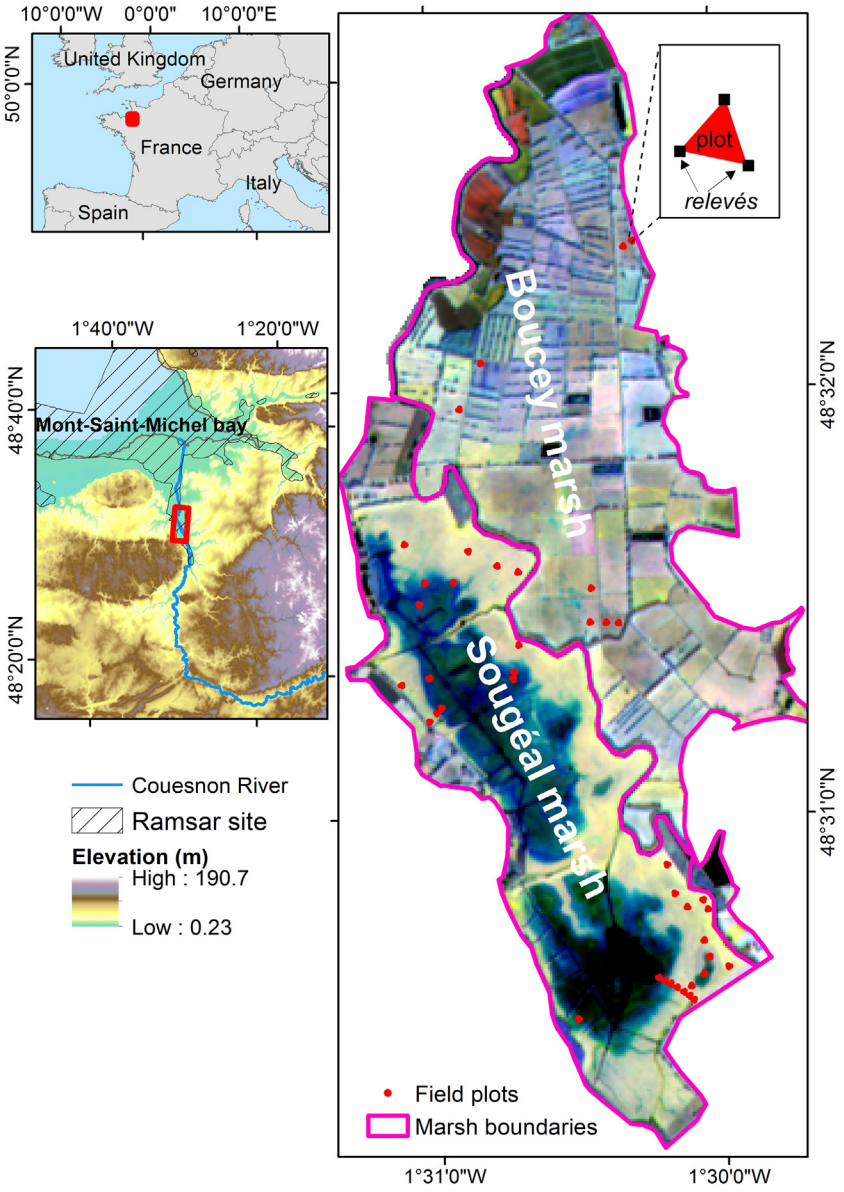

Fig. 1. Study site location and distribution of field vegetation plots. Color composite of Sentinel-2 time-series (©ESA): blue = band 8, 22 May 2017; green = band 8, 9 Apr 2017 and red = band 8, 13 Mar 2017. (For interpretation of the references to color in this figure legend, the reader is referred to the web version of this article.)

López et al. (2014) obtained a Kappa index of ~0.5 using a Landsat-5 TM image, while Kumar and Sinha (2014) achieved an overall accuracy of 42% using a Quickbird image. However, plant communities can be accurately mapped using single-date hyperspectral imagery (Burai et al., 2015; Roelofsen et al., 2014), but its expensive acquisition costs limit its application to small sites. The reflectance of plant communities measured with very high spatial resolution images is also associated with standing biomass, soil cover, and water content (Feilhauer and Schmidtlein, 2011). In addition, plant communities are distributed in small patches with similar physiognomy, which smooths out the spectral variability between them (Rocchini et al., 2013) making their discrimination using cost-effective and single-date remote sensing imagery data challenging. To address this issue, recent studies have highlighted advantages of very high spatial resolution time-series for mapping plant communities, not directly from specific plant species' spectral reflectance, but indirectly from phenology seasonality or flood duration. For example, a phenology seasonality criterion was used to discriminate plant communities from field spectroscopy time-series (Bratsch et al., 2016; Féret et al., 2015), multispectral RapidEye time-series (Schuster et al., 2015) and bi-seasonal Worldview-2 imagery (Tomaselli et al., 2016), while a flood duration criterion derived from TerraSAR-X time-series was relevant for mapping wet grassland communities (Betbeder et al., 2015). However, repeated acquisition of such remote sensing data remains expensive for scientists and environmental managers and precludes their application to larger sites.

The method used to classify remote sensing data also influences the accuracy of the vegetation map (Maxwell et al., 2018). Among the multitude of existing classifiers, the literature indicates the superiority of a machine learning classifier over a traditional parametric classifier (Khatami et al., 2016), especially when the sample size is small (Burai et al., 2015; Sanchez-Hernandez et al., 2007). Accordingly, the performance of machine learning classifiers relies upon a reliable tuning configuration (Mahdavi et al., 2017). Support vector machine (SVM) is the machine learning classifier most commonly used for remote sensing mapping and is well suited for a sparse calibration dataset with no underlying assumptions of statistical distribution (Mountrakis et al., 2011). Another popular machine learning classifier is random forest (RF), which constructs decision trees and can manage many variables

(Mutanga et al., 2012).

In recent years, the Sentinel-2 mission, which is based on a constellation of two satellites (Sentinel-2A and Sentinel-2B, launched in 2015 and 2017, respectively), continuously and extensively monitor the Earth with a high temporal frequency (revisit time of 10 days). Sentinel-2 sensors acquire multispectral images in 13 bands. These freely available data, with unprecedented fine spatial, spectral, and temporal resolutions, have great potential for wide use by environmental managers to monitor plant biodiversity. Recent studies indicate a great advantage of Sentinel-2 data for mapping tree species (Förster et al., 2017; Immitzer et al., 2016; Karasiak et al., 2017; Ng et al., 2017), but their application to mapping grassland habitats remains poorly investigated. Recently, Shoko and Mutanga (2017a) showed advantages of a single-date Sentinel-2 image for mapping two herbaceous growth patterns (i.e. C3 and C4 grasses) and encouraged future research to investigate the use of Sentinel-2 time-series to discriminate grass species.

The aim of this study was to assess the potential of Sentinel-2 time-series for discriminating plant communities in wet grasslands. We hypothesized that wet grassland plant communities can be discriminated based on their specific phenological phases and flood durations. In this study, we compared an annual time-series to single-date Sentinel-2 multispectral imagery. We defined a detailed plant community typology based on field sampling. We classified remote sensing data with the most efficient machine-learning algorithms. The strengths and shortcomings of the methods implemented are then discussed.

2. Materials and methods

2.1. Study site

The study focuses on a 475 ha site in the Couesnon floodplain, near Mont-Saint-Michel Bay, in the long-term ecological research network “ZA Armorique”, France (48°32′0″N, 1°31′0″W). This site is included within the boundaries of European Union Natura 2000 (1992/43/EEC) and international Ramsar environmentally protected areas. The topography is flat, with elevation ranging from 6 to 7 m NGF (“Nivellement Général de la France”, the elevation above the mean Mediterranean Sea level). Land cover in the floodplain consists of wet grasslands. The study site includes two distinctive marshes separated by the Couesnon River (Fig. 1): the Sougéal marsh (203 ha) on the western side of the river and the Boucey marsh (272 ha) on the eastern side of the river. The two sites differ in agricultural and water management. Sougéal marsh is designated for biological conservation: managers retain flood inflow in the marsh for water birds and pike reproduction. Agricultural activities include cattle grazing from March to November (Fig. 2). Boucey marsh includes less extensive farming, with intensive drainage throughout the year. Grasslands are managed exclusively for mowing or alternate grazing/mowing cycles. Few crops are grown in the northern portion of Boucey marsh. Although the two marshes have similar vegetation physiognomy (i.e. grasslands), many distinctive plant communities are distributed according to flood duration and agricultural practices.

2.2. Satellite data pre-processing

2.2.1. Acquisition of remote sensing data

We looked for Sentinel-2 images that were cloud-free, at least in the study area, during an annual vegetation cycle. A time-series of 12 Sentinel-2 images from 3 November 2016 to 27 August 2017 was obtained from the French space agency (CNES) website (theia.cnes.fr) (Fig. 2). All images were acquired by the Sentinel-2A sensor, except for that from 6 July 2017 (Sentinel-2B sensor). The images were geometrically rectified, and pixel values were converted into surface reflectance (Level 2) using the multi-sensor atmospheric correction and cloud screening algorithm (MAACS) (Hagolle et al., 2015). Sentinel-2 images included four spectral bands at 10 m spatial resolution in blue (b2: 497 nm), green (b3: 560 nm), red (b4: 664 nm), and infrared (b8: 835 nm) spectra. They also included six bands at 20 m spatial resolution in red-edge (b5: 704 nm, b6: 740 nm, b7: 782 nm), near-infrared (NIR) (b8a: 865 nm), and short-wave infrared (SWIR) (b11: 1614 nm, b12: 2202 nm) spectra. The three atmospheric bands (b1, b9 and b10) were excluded from the analysis.

2.2.2. Resampling and stacking Sentinel-2 images

The 20 m bands of each Sentinel-2 image were subsampled to a 10 m grid using the nearest neighbor approach. Then, these subsampled bands were stacked with the other 10 m bands (b2, b3, b4 and b8) into a temporary raster file. Finally, the 12 images were stacked into a matrix raster with 120 layers at a 10 m spatial resolution to obtain the correct format for classification analysis.

2.3. Analysis of vegetation data

2.3.1. Field sampling

Vegetation relevés were collected from May to June 2017 during the annual vegetation peak. To fit with the 10 m spatial resolution of Sentinel-2 imagery, field sampling was done in patches larger than 100 m^2 with an *a priori* homogeneous plant community. Homogeneous vegetation patches were visually identified based on the identification of dominant species and consistent micro-topography. Next, plots were established (each an equilateral triangle with 10 m sides), and vegetation relevés in 2 m × 2 m areas were carried out in each angle of the triangle. For each vegetation relevé, the traditional phytosociological protocol was applied. An exhaustive inventory of plant species with their abundance expressed using the Braun-Blanquet index was conducted. The center of each relevé was geo-referenced using differential GPS (horizontal accuracy < 0.5 m). Jaccard and Sorensen species dissimilarity indices were calculated for the three relevés in each plot to confirm the homogeneity of species composition (Table A1). Finally, 123 vegetation relevés from 41 plots were collected and input into the TURBOVEG vegetation database (Hennekens and Schaminée, 2001). TURBOVEG is a comprehensive database management system designed for the storage, selection, and export of vegetation data (relevés). One of its advantages is that it checks and corrects the taxonomy of plant species based on the French national reference TAXREF (Gargominy et al., 2012).

2.3.2. Unsupervised classification of vegetation relevés

We developed a typology of plant communities *via* an unsupervised classification of the vegetation relevés based on their species composition. To group these vegetation relevés into consistent clusters (i.e. plant communities), a numerical approach was applied using JUICE software (Tichý, 2002). Unsupervised classification of each relevé was conducted using the modified hierarchical TWINSPAN algorithm (Hill, 1979). We applied the TWINSPAN classification to the 123 vegetation relevés rather than the 41 averaged plots to preserve the variance of the data. The TWINSPAN algorithm was run with default parameter settings (i.e. pseudospecies cut level: 3; values of cut levels: 0, 5, 25; minimum group size: 3). The final number of divisions was chosen based on expert-based validation. The compactness and distinctiveness of clusters were statistically assessed using the average silhouette width (Kaufman and Rousseeuw, 1990), a standard measure of cluster isolation. Specifically, the silhouette width, ranging from −1 to 1, is a measure of how similar a vegetation relevé is to its clusters, with negative values indicating misclassified relevés. For each plot, we assigned the majority cluster label to its 3 constituent relevés (Table B1). A summary table, which describes the percentage frequency of each species per cluster, was created, and correspondence between clusters and European Nature Information System (EUNIS) habitat types (Davies et al., 2004) was determined for clearer interpretation.

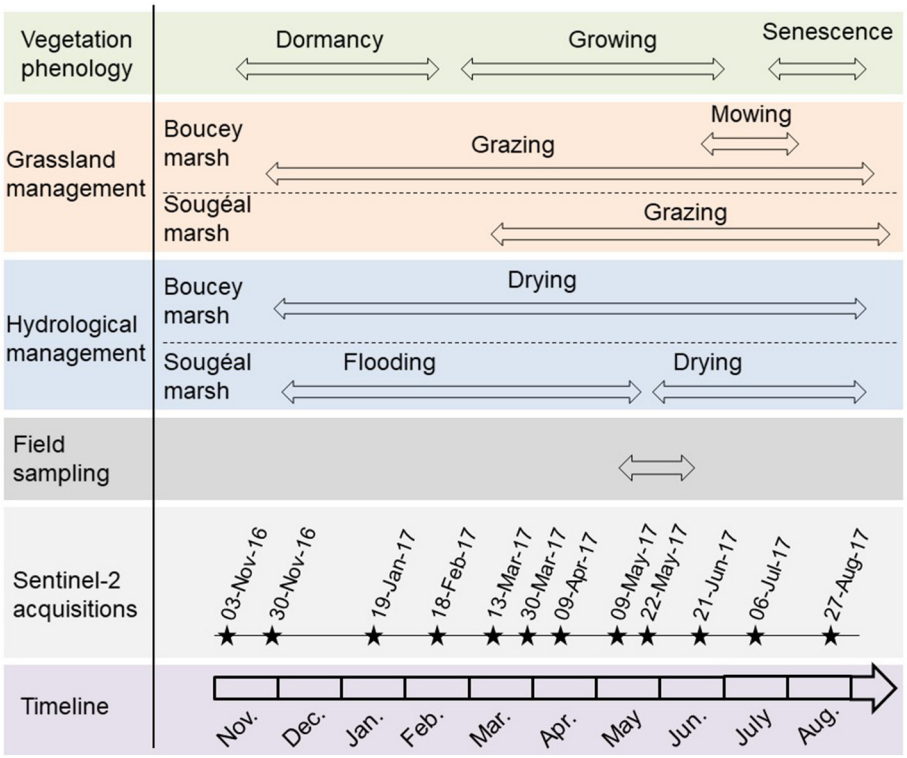

Fig. 2. Sentinel-2 acquisition dates in relation to vegetation phenology, grassland management and hydrological management of the Couesnon marshes.

2.4. Analysis of satellite data

2.4.1. Creation of spectral signature files

The sample plot vector layer and the Sentinel-2 time-series were subsequently overlaid in a GIS environment. Pixels included in at least 1/3 of plot areas were manually selected in each dataset. Then, the median spectral value of each band was assigned to the plot.

2.4.2. Dimension reduction

Because the Sentinel-2 time-series contained many spectral bands (n = 12 dates × 10 bands), the number of dimensions was decreased using recursive feature elimination (RFE) to retain the most discriminating bands. We applied the well-established RFE method developed by Kuhn (2012) and implemented in the R package "caret" using an SVM algorithm with 10 repeated 3-fold cross-validation. Variation in classification accuracy that considered the number of spectral bands of the Sentinel-2 time-series selected retained 26 of the 120 bands (Fig. C1).

2.4.3. Supervised classification

We mapped plant communities through supervised classification of the Sentinel-2 images, using the spectral values of the 41 field plots as basis for the model calibration. Two machine learning classifiers, SVM (with a linear and radial kernel) and RF, were applied to the Sentinel-2 time-series data and subsequently to the 12 single-date dataset (i.e. the 10 spectral bands from each date) and the 10 single-band dataset (i.e. the 12 dates for each spectral band), which were then compared. Classification models were calibrated and validated using 10 repeated 3-fold cross-validation. More folds were not possible due to the sparse calibration dataset (n = 41). For the Sentinel-2 time-series classification, the SVM algorithm was applied to the 26 most discriminating spectral bands assigned from the RFE, while the RF algorithm, which included an internal band selection procedure, was applied to all 120 spectral bands. A mean overall accuracy (OA) index and a Kappa index (and their respective standard deviations (SD)) were calculated for each remote sensing dataset and for each classifier. A cross-validated confusion matrix representing the error distribution per class among the 10 repeats was performed for the Sentinel-2 time-series classification to obtain the most accurate classifier. A map of grassland plant communities was derived from the classification of Sentinel-2 time-series: non-wetland and non-grassland areas were masked using ancillary thematic layers (Inglada et al., 2017; Rapinel et al., 2015b).

All remote sensing analyses were performed in the R 3.4.3 statistical environment (R. Core Team, 2017) using the packages "raster" v 2.6–7 (Hijmans, 2015) and "caret" v 6.0–79 (Kuhn, 2008).

3. Results

3.1. Floristic typology

The 123 vegetation relevés were clustered using TWINSPAN into seven plant communities. The quality of clustering was considered satisfactory given the positive average silhouette widths (Fig. D1). The seven plant communities were distributed along flood duration and grazing gradients (Table 1). All plant communities belonged to EUNIS E2.2 (low and medium elevation hay meadows) and E3.4 (seasonally wet and wet grasslands) classes.

Plant communities 1–4 were distributed on mesophilic grasslands, but could be distinguished by their grazing intensity. Plant community 1 was associated exclusively with mown grasslands, with typical species such as *Arrhenatherum elatius* and *Festuca arundinacea*. Plant community 2 was found on grasslands with alternate of grazing and mowing, with *Anthoxanthum odoratum* and *Bromus racemosus* species. Plant communities 3 and 4 were floristically similar and were located on more continuously grazed grasslands. Plant community 3 was characterized by *Holcus lanatus*, while plant community 4 was distributed in moister mesophilic grasslands characterized by *Poa trivialis*, *Cirsium arvense* and *Trifolium repens*. Plant community 5 corresponded to meso-hygrophilic (i.e. transitional area between mesophilic and hygrophilic grasslands) and grazed grasslands. Its species composition was characterized by *Alopecurus geniculatus*, *Oenanthe fistulosa* and *Eleocharis acicularis*. Plant communities 6 and 7 were floristically similar and representative of

Table 1
Summary table of the grassland plant communities in the Couesnon marshes. Percentage frequency values of species in each plant community are derived from TWINSPAN classification. Higher values are indicated in gray (≥60) and dark gray (≥80).

Plant community number	1	2	3	4	5	6	7
Number of relevés	6	15	23	35	24	12	8
Arrhenatherum elatius	100	–	–	–	–	–	–
Festuca arundinacea	100	7	4	–	–	–	–
Festuca rubra	83	–	–	–	–	–	–
Rumex acetosa	67	47	–	–	–	–	–
Trifolium pratense	67	40	–	–	–	–	–
Lathyrus pratensis	67	–	–	–	–	–	–
Leontodon autumnalis	67	40	–	–	–	–	–
Anthoxanthum odoratum	–	93	4	–	–	–	–
Ranunculus acris	50	80	–	9	–	–	–
Bromus racemosus	–	80	–	–	–	–	–
Alopecurus pratensis	–	60	39	20	4	–	–
Cirsium arvense	–	–	35	69	21	–	–
Oenanthe fistulosa	–	–	–	6	92	25	25
Eleocharis acicularis	–	–	–	6	83	17	13
Cardamine pratensis	–	20	4	6	75	–	13
Potentilla anserina	–	13	–	23	75	8	13
Ranunculus flammula	–	–	–	3	42	83	25
Eleocharis palustris	–	–	9	–	42	83	–
Veronica scutellata	–	–	–	–	–	8	75
Lemna minor	–	–	–	–	–	25	63
Hydrocotyle vulgaris	–	–	–	–	4	–	63
Holcus lanatus	100	53	96	26	–	–	–
Plantago lanceolata	100	67	–	–	–	–	–
Taraxacum officinale	83	100	–	–	–	–	–
Rumex crispus	17	–	61	51	67	–	–
Trifolium repens	17	–	4	71	83	–	–
Carex hirta	–	33	30	60	71	8	–
Alopecurus geniculatus	–	–	4	14	100	75	38
Glyceria fluitans	–	–	4	–	54	92	100
Galium palustre	–	7	–	–	38	83	88
Lolium perenne	33	87	65	89	21	–	–
Persicaria amphibia	–	–	–	3	75	83	75
Poa trivialis	67	87	65	91	50	–	–
Ranunculus repens	67	93	78	63	88	8	–
Agrostis stolonifera	50	100	100	100	88	83	75

hygrophilic and grazed grasslands. However, few differences were observed in species composition: *Ranunculus flammula* and *Eleocharis palustris* were often observed in plant community 6 but not in plant community 7.

3.2. Mapping plant communities

A plant community map was derived successfully from the Sentinel-2 time-series regardless of the classifier used. In detail, the OA of the classification of the full Sentinel-2 time-series assessed from 10 repeated 3-fold cross-validation ranged from 0.71 ± 0.08 (Kappa index = 0.63 ± 0.09) for the RF classifier to 0.77 ± 0.06 (Kappa index = 0.72 ± 0.07) and 0.78 ± 0.05 (Kappa index = 0.73 ± 0.06) for the SVM classifier with a radial and linear kernel, respectively. This highlights the slight influence (Δ = 0.07) of the classifier on OA. Analysis of the confusion matrix for the SVM classifier with a linear kernel (Table 2) shows that misclassification errors occurred mainly within plant communities with similar species composition (e.g. plant community 3 vs. plant community 4, plant community 5 vs. plant community 6). Underdetection and overdetection errors were

Table 2
Cross-validated (3-fold, repeated 10 times) confusion matrix between the support vector machine classification (linear kernel) of plant communities derived from the Sentinel-2 time-series (lines) and field plots (columns). Entries are percentages of average cell counts among repeats. The percentages of overdetection (OD) and underdetection (UD) are given for per plant community.

		References							
Prediction: Class name		1	2	3	4	5	6	7	OD
Plant community 1	1	4.5			0.7				**13**
Plant community 2	2	0.2	11.9	1.4	0.5				**15**
Plant community 3	3			11.7	3.1				**21**
Plant community 4	4	2.4		2.9	24.3	2.4			**24**
Plant community 5	5			0.7		13.8	2.1	2.1	**26**
Plant community 6	6						7.1		**0**
Plant community 7	7					2.9	0.2	5.0	**38**
	UD	**37**	**0**	**29**	**15**	**28**	**24**	**30**	

Accuracy (average) 0.78
Kappa (average) 0.73

acceptable (≤30%) for all plant communities except plant community 1 and plant community 7, which were influenced by moderate underdetection (37%) and overdetection errors (38%), respectively. Conversely, plant community 2 was classified with greater accuracy since the under- and overdetection errors were < 15%.

The map of plant communities derived from the Sentinel-2 time-series classification (Fig. 5) highlights a clear difference in plant community composition between the two marshes, which agreed with their hydrological and grassland management. Plant communities 1 and 2 - typical of mesophilic and mown grasslands - were abundantly present in Boucey marsh (33% and 44% of total grassland area, respectively) but absent in Sougéal marsh (2% and 5% of total grassland area, respectively). Conversely, plant communities 5, 6, and 7 - indicators of long-flooded and grazed grasslands - were well distributed in Sougéal marsh (21%, 14%, and 15% of total grassland area, respectively) but were rarely mapped in Boucey marsh (1%, 3%, and 0% of total grassland area, respectively). Plant communities 3 and 4 - indicators of mesophilic and grazed grasslands - were located on the alluvial ridge (higher elevations) of the Couesnon River.

3.3. Importance of date and spectral band to discriminating plant communities

The influence of date and spectral band on the classification accuracy of plant communities is shown in Figs. 3 and 4, respectively. OA was lower and varied significantly (Δ = 0.34) when using a single-date Sentinel-2 image. Accuracy was lowest during periods of vegetation dormancy (3 November 2016 to 18 February 2017) and senescence (6 July to 27 August 2017), while it was highest during the growing period (9 April to 21 June 2017). Specifically, maximum accuracy was 0.67 ± 0.07 (Kappa index = 0.59 ± 0.09) on 9 May 2017, while minimum accuracy did not exceed 0.33 ± 0.11 (Kappa index = 0.17 ± 0.13) on 30 November 2016 with the linear SVM classifier.

Unlike the date, the spectral band had a slight influence on variation in accuracy (Δ = 0.12). Accuracy was lowest in the b2 (blue) band (0.58 ± 0.12, Kappa index = 0.49 ± 0.15), while it was highest in the b3 (green) band (0.70 ± 0.10, Kappa index = 0.63 ± 0.12) with the linear SVM classifier. Interestingly, b5 and b6 (red edge), b8 and b8a (IR), and b11 and b12 (SWIR) bands had similar accuracies, ranging from 0.60 (Kappa index = 0.49) to 0.65 (Kappa index = 0.57).

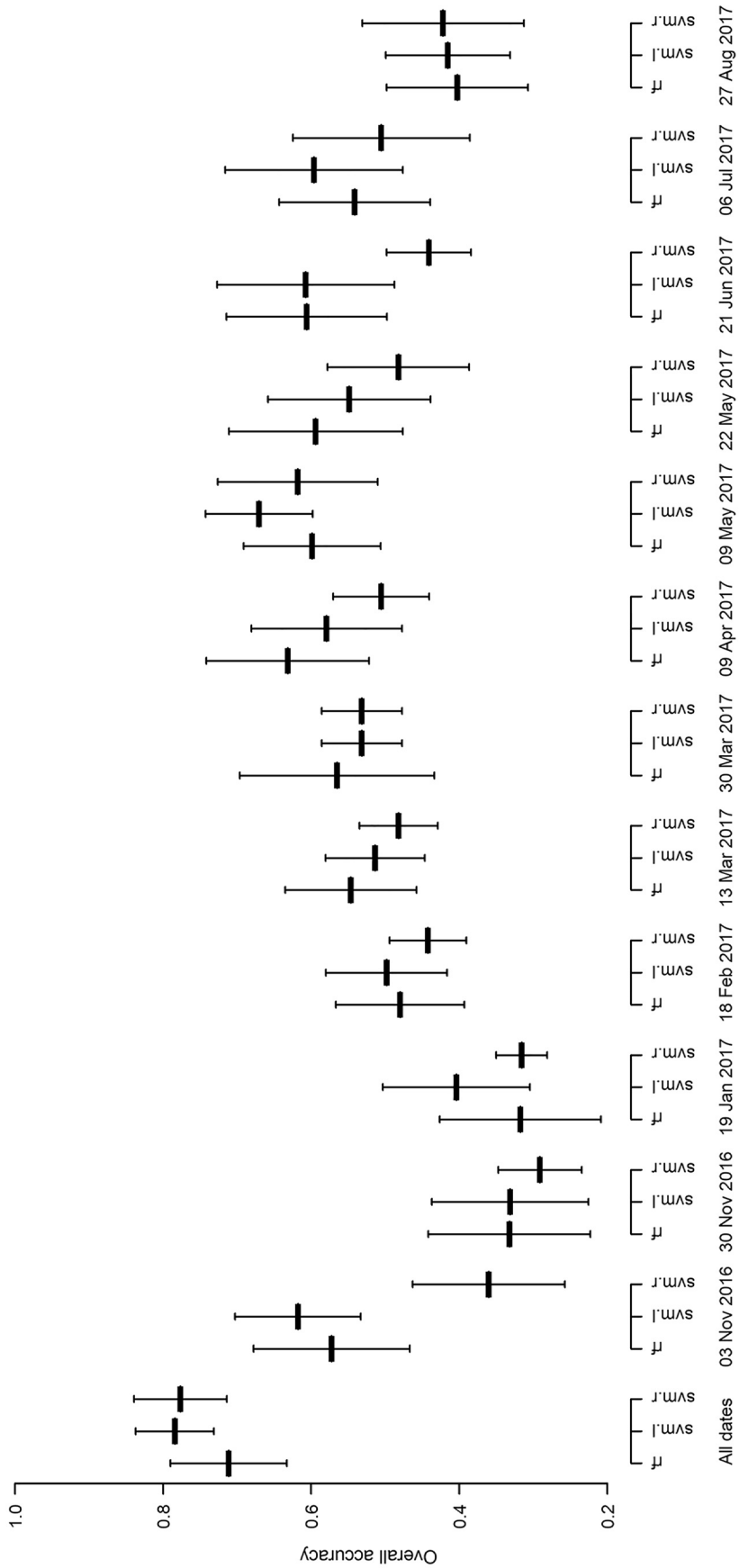

Fig. 3. Influence of date on Sentinel-2 image classification accuracy per classifier (rf = random forest; svm.l = support vector machine (SVM) with a linear kernel; svm.r = SVM with a radial kernel). Whiskers indicate the standard deviation of cross-validation replicates.

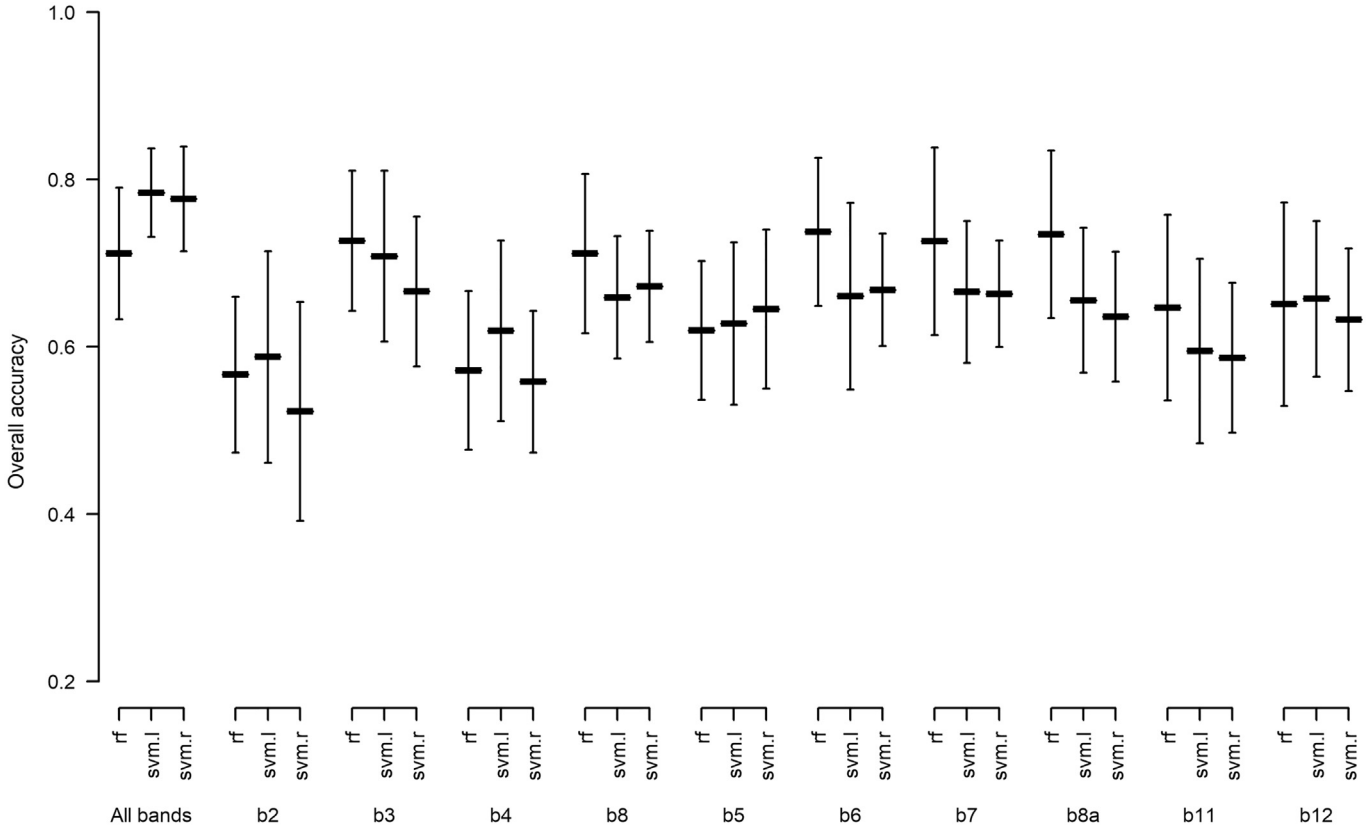

Fig. 4. Influence of spectral band on Sentinel-2 image classification accuracy per classifier (rf = random forest; svm.l = support vector machine (SVM) with a linear kernel; svm.r = SVM with a radial kernel). Whiskers indicate the standard deviation of cross-validation replicates.

4. Discussion

4.1. Advantages of Sentinel-2 time-series for mapping grassland plant communities

Sentinel-2 time-series, which combine high temporal, spectral and spatial resolutions, provide an unprecedented view of impacts of hydrological and grassland management on the distribution of grassland plant communities in the Couesnon marshes. Although Shoko and Mutanga (2017a) highlighted the advantages of one single-date Sentinel-2 imagery for mapping two herbaceous growth patterns, our study goes further and demonstrates that a cost-effective Sentinel-2 time-series can accurately map seven grassland plant communities (OA = 0.78, Kappa index = 0.73). Previous studies reached similar accuracies, but used expensive remote sensing data such as airborne hyperspectral imagery (Burai et al., 2015; Neumann et al., 2015; Oldeland et al., 2010), TerraSAR-X time-series (Schuster et al., 2015), full-waveform LiDAR data (Zlinszky et al., 2014), or an unmanned aerial vehicle (Kaneko and Nohara, 2014). Our analyses based on real Sentinel- 2 satellite time-series confirm preliminary studies which showed the potential of field-spectra-simulated Sentinel-2 time-series for discriminating natural grasslands (Feilhauer et al., 2013; Féret et al., 2015).

Facies of plant communities vary throughout the year according to the specific phenology of each plant species. Most of the time, grassland plant communities have similar physiognomy that smooths the spectral difference between them (Rocchini et al., 2013); however, they can appear distinct during a brief period (Feilhauer et al., 2013). Hence, multi-temporal Sentinel-2 data has great value in identifying these phenological differences; for example, *Festuca* and *Themeda* grass species were clearly discriminated in summer but not in winter Sentinel-2 images (Shoko and Mutanga, 2017a, 2017b). In our study, plant communities 5 and 6 were correctly discriminated from the Sentinel-2 time-series (only 2.1% of error between them, Table 2) despite having similar floristic composition and both growing on long-flooded and grazed grasslands. This low error may be due to the yellow flowers of *Ranunculus flammula* (42% and 83% frequency in plant community 5 and 6, respectively) in April and the white flowers of *Oenanthe fistulosa* (92% and 25% frequency in plant community 5 and 6, respectively) from May–June.

The Sentinel-2 sensor provides spectral bands with a 10 or 20 m spatial resolution, which is coarser than the fine-grained pattern of grassland plant communities (Marion et al., 2010). As suggested by Roth et al. (2015), classification of Sentinel-2 time-series represents only a coarse grain pattern of vegetation patches, in which small, long or thin patches cannot be discerned. A higher spatial resolution (2–5 m) would be more appropriate for the fine-grained pattern of grassland plant communities. Merging Sentinel-2 images with very high spatial resolution satellite images is a potential solution for capturing small plant community patches (Pereira et al., 2017), although it requires multiple acquisitions at the higher resolution for each low-resolution image (Chen et al., 2015).

Field vegetation plots were sampled from May–June 2017 to calibrate Sentinel-2 time-series acquired from November 2016 to August 2017. Unlike functional properties of vegetation (e.g. biomass, nitrogen content), which evolve rapidly, the structural composition of vegetation evolves more slowly (over ± 2 years) (Dumont et al., 2012). As a result, a one-year shift between field sampling and remote sensing data acquisitions appears acceptable for classifying vegetation. Since the remote sensing sensor does not adequately characterize vegetation when grasslands have been recently mown or flooded, images should be acquired during the period of peak vegetation when using a single-date image (Feilhauer et al., 2013; Schmidtlein et al., 2007; Zlinszky et al., 2014). This is less true for remote sensing time-series, in which

detection of flooded or mown grassland can be a good proxy for characterizing hydrological management (Betbeder et al., 2015) and grassland management (Franke et al., 2012) and *in fine* for discriminating natural vegetation units. Beyond differences in phenology, the flood duration criterion helped to discriminate flooded plant communities (5, 6, and 7) from non-flooded plant communities (1 and 2), mainly located in Sougéal and Boucey marshes, respectively, while discrimination among non-flooded plant communities (1, 2 and 3) within Boucey marsh was due to differences in grassland management.

4.2. Influence of date, spectral band, and classifier on plant community discrimination

We show that classification of Sentinel-2 time-series is more accurate (OA = 0.78, Kappa index = 0.73) than those derived from a single-date Sentinel-2 image (maximum OA = 0.67, Kappa index = 0.59) or from a single-band Sentinel-2 image (maximum OA = 0.70, Kappa index = 0.63). We also highlight that date had a greater influence than spectral band on classification accuracy (Δ = 0.34 and 0.12 in OA, respectively). These results confirm the assumption of Schuster et al. (2015), who argued that high temporal resolution is more important than sensor characteristics. More precisely, we show spring/early summer (9 April 2017 to 21 June 2017) is the most informative period for discriminating plant communities. Previous remote sensing-based studies also indicated that this period is crucial and involves many criteria, such as flood duration (Betbeder et al., 2015), plant phenology (Franke et al., 2012; Schuster et al., 2015), and the annual vegetation peak (Feilhauer et al., 2013; Féret et al., 2015; Schmidt et al., 2014; Shoko and Mutanga, 2017b). From an ecological viewpoint, this period is considered a “hot moment” because it is when (1) wet marshes dry quickly within a few weeks, yielding clear spatial patterns due to flood duration (Rapinel et al., 2018), and (2) wet grassland vegetation reaches the annual peak in plant development (Maltby and Barker, 2009). Accordingly, the timing and extent of this “hot moment” for discriminating plant communities may shift from year-to-year depending on climate variations, as well as local hydrological and grassland management.

Although previous studies indicated that spectral band, such as red-edge (Robinson et al., 2016; Shoko and Mutanga, 2017a), NIR (Feilhauer et al., 2013), and SWIR (Davranche et al., 2010; Jacob et al., 2014), had a clear influence on discrimination of natural vegetation, spectral band influenced OA only slightly (Δ = 0.12) in our study. This could have been due to our having considered each spectral band over all dates in the time-series, which could have “smoothed” differences among the bands.

Our results showed that the SVM classifier slightly outperformed the RF classifier (Δ = 0.07 in OA). Based on the 10 repeated 3-fold cross-validation (i.e. 30 replicates), we calculated a small SD for both classifiers (± 0.06). These results should be compared to those of previous studies cautiously, since procedures (e.g. cross-validation type, sample size, hyperparameter tuning) may differ (Maxwell et al., 2018). That said, our results are similar to those of Burai et al. (2015) and Maxwell et al. (2014), who highlighted that SVM outperformed RF by ~0.03 in OA. Conversely, Adam et al. (2014) claimed that RF performed better than SVM by ~2%, while Duro et al. (2012) concluded that results of RF and SVM classifiers did not differ statistically.

4.3. Methodological considerations

Vegetation relevés were collected in floristically homogeneous patches that were visually delineated in the field based on identifying dominant plant species and consistent micro-topography. Since plant communities in wet grasslands are distributed mainly in fine-grained patterns (Marion et al., 2010), delineating large patches (> 100 m^2) that met the required Sentinel-2 pixel size was challenging and time-consuming. Nearly 80 h of fieldwork by two experienced scientists (including automobile driving, identification of vegetation patches, and plant species inventories) were required to collect the 123 vegetation relevés from 41 plots on a well-known study site. This limitation should be considered when planning a field campaign, even when using very high spatial resolution (2 cm) unmanned aerial vehicle imagery, which can help identify large and floristically homogeneous patches locally (Yoshino et al., 2014). One limitation of the fieldwork was the short duration (only 2 months: May–June) of peak vegetation growth during which vegetation relevés can be collected. Specifically, we expected to perform more relevés in Boucey marsh, but some grasslands had already been mown in June.

We defined a detailed habitat typology to explore the ability of the Sentinel-2 time-series in depth. Existing habitat typologies (e.g. CORINE Biotope, EUNIS, Natura 2000) are considered too broad and inconsistent for European grassland plant communities (Dengler et al., 2013). Consequently, we defined our typology using an unsupervised hierarchical TWINSPAN classifier based only on our dataset of vegetation relevés. The summary table (Table 1) and silhouette index (Fig. D1) indicate consistent vegetation units in the local context of grasslands in the Couesnon marshes. However, the sparse vegetation dataset and small study site area (480 ha) may reduce the significance and robustness of this typology at the regional scale (De Cáceres et al., 2015). Integrating additional relevés from existing and comprehensive databases, such as VegFrance (Bonis and Bouzillé, 2012) or WetVegEurope (Landucci et al., 2015), and applying alternative classifiers, such as semi-supervised algorithms (Tichý et al., 2014), is a suitable solution for developing consistent classifications of European wet grassland plant communities (Dengler et al., 2013).

Extracting pure spectral signatures from vegetation plots remains challenging, especially when the pixel size is larger than field plot areas (Hauglin and Ørka, 2016). In this study, plots were designed in the form of a 10 m triangle to meet the Sentinel-2 pixel size. However, most pixels selected to calculate spectral signatures of plots could be considered “mixed pixels”, since they cover not only a part of the plot but also surrounding areas. This issue is more critical for native Sentinel-2 20 m bands resampled at a 10 m resolution. In theory, the field plot should have been > 400 m^2 to account for the 20 m Sentinel-2 bands, but in practice, this size was not feasible since patches of plant communities in grasslands were rarely so large. Nevertheless, because we carefully designed plots within floristically homogeneous patches > 100 m^2, it is reasonable to assume that species composition observed within the 10 m plots is similar to that in surrounding areas. Incidentally, Jaccard and Sorensen dissimilarity indices of plant species per plot tended to have low values (Table A1). An attractive alternative is to downscale the vegetation unit from a single plant community to a set of plant communities (Biondi et al., 2011) to conform to the 20 m Sentinel-2 bands. This approach was successfully applied to Atlantic saltmarshes using 30 m Landsat bands (Rapinel et al., 2015a) and merit assessment with 10–20 m Sentinel-2 bands and the future EnMAP (Environmental Mapping and Analysis Program) hyperspectral images.

Despite substantial fieldwork, the number of field plots was small (n = 41) given the number of grassland plant communities (n = 7). Therefore, overfitting was a legitimate concern. Unbiased and robust performance evaluation is an important issue in machine learning research (Cawley and Talbot, 2010). Robustness is influenced by overfitting, which occurs when a model fits the training data well but is not generalizable (Maxwell et al., 2018). In other words, overfitting results in estimated accuracy that has low bias (i.e. expected difference with actual accuracy) but high variability (Wong, 2015). One obvious way to detect overfitting is to use an independent test set. However, although pre-existing vegetation plots were surveyed in 2008 in this long-term ecological research network study site, we could not use them as an independent validation dataset to assess the SVM and RF models since plant communities' patterns may have changed within a decade. Even if we could have done so, we would likely have used them to increase accuracy of the models. Instead, we used 10 repeated 3-fold cross-

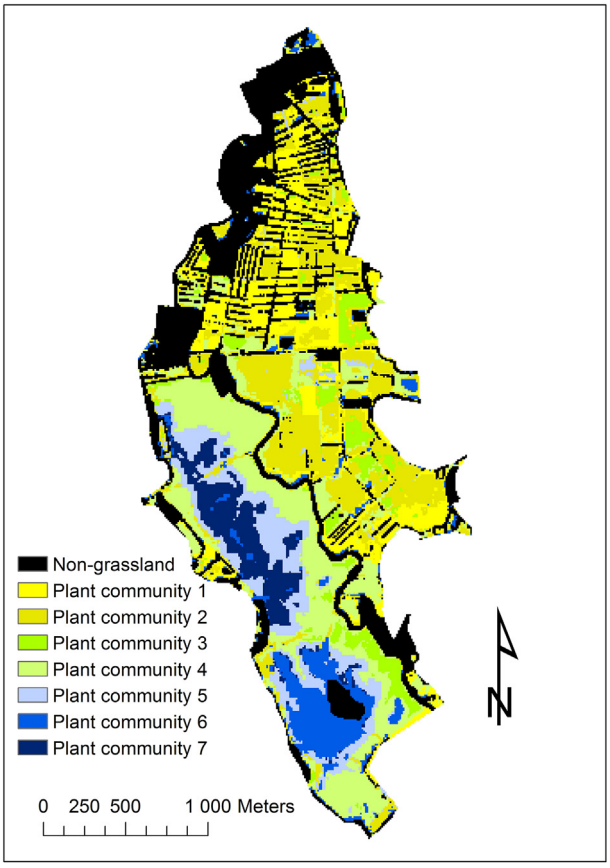

Fig. 5. Map of plant communities derived from the classification of Sentinel-2 time-series using a linear kernel support vector machine classifier.

validation to provide reasonable estimates of the expected error (Kuhn and Johnson, 2013). Our statistical results - based on 30 replicates - showed not only moderate average bias (0.22 in OA) but also low variability (± 0.07). Accordingly, our small number of field plots (n = 41) resulted in overlapping training and test datasets during the cross-validation procedure and *in fine* an underestimate of the variability (Refaeilzadeh et al., 2009; Wong, 2015). Beyond statistical validation, model robustness can be qualitatively assessed using the map that results from applying the model to all pixels (Correll et al., 2018): visual interpretation of the Sentinel-2 classification revealed consistent spatial distribution of plant communities in the marshes (Fig. 5).

In accordance with previous studies (Burai et al., 2015; Karasiak et al., 2017), our results highlighted that the SVM classifier consistently outperformed the RF classifier in OA (± 10 percentage points). However, the accuracy of SVM classification could be increased; we used a traditional approach to analyze the Sentinel-2 time-series: the 120 spectral bands were stacked in one file and classified with classic kernels that ignored the chronological order of the time-series. In contrast, temporal kernels - such as dynamic time warping - have been shown to help identify grassland management from remote sensing time-series (Dusseux et al., 2013) and appear a promising solution for monitoring plant communities from Sentinel-2 time-series. Nevertheless, temporal kernels are better suited for comparing time-series with > 20 points/images (Betbeder et al., 2014), while our annual Sentinel-2 time-series contained only 12 images. Betbeder et al. (2014) compared linear and temporal kernels to map natural wet grasslands using 6 SAR images and found that the linear kernel significantly outperformed the temporal kernel (Kappa = 0.73 and 0.32, respectively). Considering a longer period (2 years) and/or merging Sentinel-2 data with SAR Sentinel-1 data would result in a denser time-series that is well adapted for temporal kernels. Another alternative is to explicitly add phenological parameters based on time-series analysis of Sentinel-2 data (Vrieling et al., 2018).

Although Sentinel-2 data have great potential for the calculation of vegetation indices, we did not use vegetation indices as additional variables since they slightly increased classification accuracy compared to temporal or spectral resolutions (Khatami et al., 2016). However, vegetation indices derived from Sentinel-2 data would be useful for characterizing physical properties of vegetation in relation to functional traits, such as annual net primary production and nitrogen content (Lausch et al., 2016).

5. Conclusion

This study has demonstrated advantages of using Sentinel-2 time-series to accurately map wet grassland plant communities. Beyond phenology, mesophilic and hygrophilic plant communities were discriminated based on differences in flood duration and saturation of the topsoil, while mown and grazed plant communities were discriminated based on differences in grassland management. Discriminant analysis revealed that the spring/early summer season was the most informative period for mapping plant communities in floodplains, while spectral bands had little influence on accuracy. Sentinel-2 time-series discriminated grassland plant communities better than a single-date or single-band Sentinel-2 dataset. Future studies could focus on integrating temporal kernels in the classification process.

Acknowledgements

The authors are thankful to the European Space Agency (ESA), the Copernicus program, the French space agency (CNES) and the Theia center for providing free Sentinel-2 images. We are also grateful to the French Ministry of Ecology, Sustainable Development and Energy - CarHAB program (grant number 2101606295) - and the French National Research Center (CNRS) - Zone Atelier program - for funding the research. We would also like to thank Mireille Clément and Thomas Houet for their help in the field.

Appendix A

Table A1
Jaccard and Sorensen dissimilarity indices of plant species per plot.

	Dissimilarity index	
Plot	Jaccard	Sorensen
1	0.39	0.24
2	0.38	0.25
3	0.52	0.36
4	0.56	0.39
5	0.41	0.26

Table A1 (*continued*)

	Dissimilarity index	
Plot	Jaccard	Sorensen
6	0.41	0.27
7	0.50	0.33
8	0.66	0.51
9	0.44	0.30
10	0.46	0.30
11	0.23	0.14
12	0.38	0.24
13	0.34	0.21
14	0.32	0.19
15	0.51	0.36
16	0.27	0.16
17	0.51	0.35
18	0.31	0.19
19	0.26	0.15
20	0.33	0.20
21	0.37	0.23
22	0.44	0.29
23	0.19	0.11
24	0.47	0.32
25	0.31	0.18
26	0.39	0.25
27	0.43	0.28
28	0.50	0.34
29	0.45	0.29
30	0.50	0.34
31	0.26	0.15
32	0.17	0.10
33	0.30	0.18
34	0.35	0.21
35	0.48	0.32
36	0.60	0.44
37	0.47	0.31
38	0.39	0.25
39	0.42	0.27
40	0.59	0.42
41	0.41	0.26

Appendix B

Table B1
List of cluster labels per relevé and plot (Microsoft® Excel file).

Plot ID	Relevé ID	Relevé cluster label	Plot cluster label
1	1	2	2
	2	2	
	3	2	
2	4	2	2
	5	2	
	6	2	
3	7	2	2
	8	2	
	9	2	
4	10	2	2
	11	2	
	12	2	
5	13	1	1
	14	1	
	15	1	
6	16	1	1
	17	1	
	18	1	
7	19	2	2
	20	2	
	21	2	
8	22	3	3
	23	3	
	24	3	
9	25	4	4
	26	4	
	27	4	

(*continued on next page*)

Table B1 (*continued*)

Plot ID	Relevé ID	Relevé cluster label	Plot cluster label
10	28	3	3
	29	3	
	30	3	
11	31	3	3
	32	3	
	33	3	
12	34	3	3
	35	3	
	36	3	
13	37	3	3
	38	3	
	39	3	
14	40	4	4
	41	4	
	42	4	
15	43	4	4
	44	4	
	45	4	
16	46	4	4
	47	4	
	48	4	
17	49	3	4
	50	4	
	51	4	
18	52	4	4
	53	4	
	54	4	
19	55	4	4
	56	4	
	57	4	
20	58	4	4
	59	4	
	60	4	
21	61	3	3
	62	3	
	63	3	
22	64	3	4
	65	4	
	66	4	
23	67	3	3
	68	3	
	69	3	
24	70	4	4
	71	4	
	72	4	
25	73	4	4
	74	4	
	75	4	
26	76	5	5
	77	5	
	78	5	
27	79	5	5
	80	5	
	81	5	
28	82	5	5
	83	5	
	84	5	
29	85	4	4
	86	4	
	87	4	
30	88	6	6
	89	5	
	90	6	
31	91	4	5
	92	5	
	93	5	
32	94	5	5
	95	5	
	96	5	
33	97	5	5
	98	5	
	99	5	
34	100	5	5
	101	5	

(*continued on next page*)

Table B1 (*continued*)

Plot ID	Relevé ID	Relevé cluster label	Plot cluster label
	102	5	
35	103	7	7
	104	7	
	105	7	
36	106	7	7
	107	7	
	108	7	
37	109	6	6
	110	6	
	111	6	
38	112	6	6
	113	6	
	114	6	
39	115	5	5
	116	5	
	117	5	
40	118	6	6
	119	6	
	120	6	
41	121	7	7
	122	7	
	123	6	

Appendix C

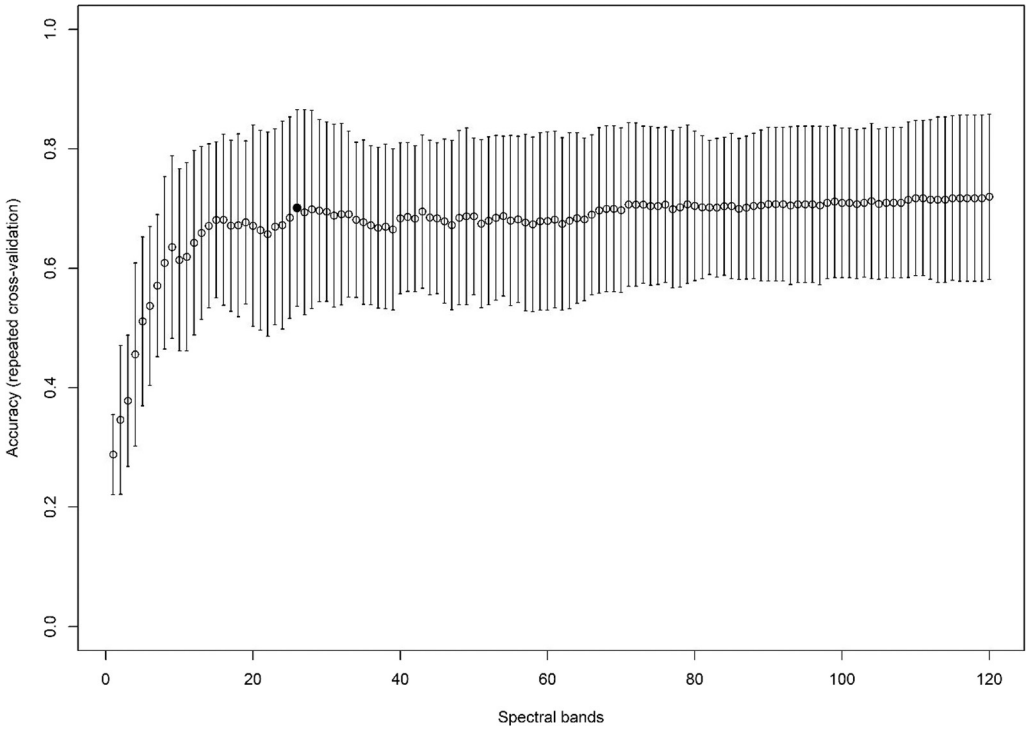

Fig. C1. Variability in classification accuracy as a function of the number of spectral bands of the Sentinel-2 time-series considered. The black dot indicates the number of variables retained for the subsequent classification process. Whiskers indicate the standard deviation of cross-validation replicates.

Appendix D

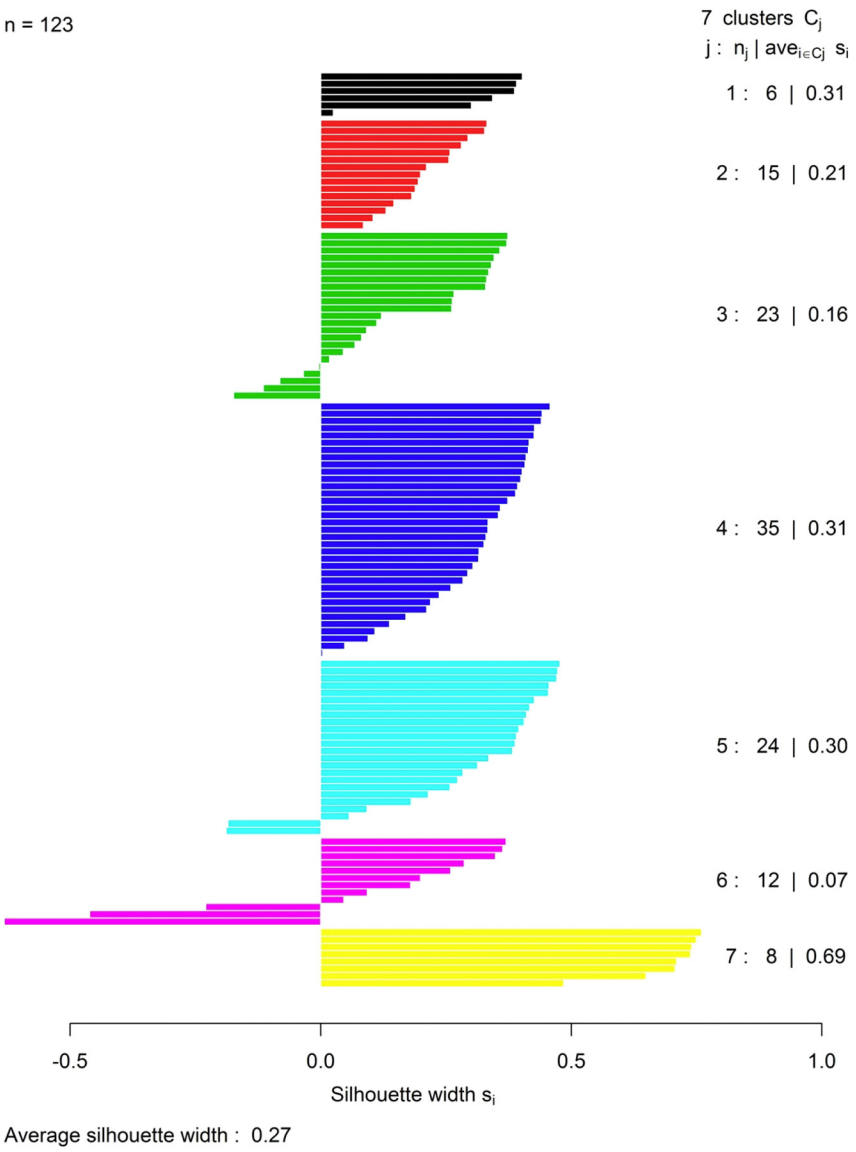

Fig. D1. Silhouette plot of the TWINSPAN classification in which each vegetation relevé is ordered according to cluster (in color) as a horizontal bar. Clusters are identified by their name j, followed by the number of relevés classified in the cluster n_j, and the average "silhouette width" by cluster $ave_{i∈Cj}$ S_i. Silhouette plots assign silhouette widths S_i to each vegetation relevé $_i$ within a cluster with a value from −1 to 1. The silhouette width is calculated by comparing a vegetation relevé 's mean similarity to other vegetation relevés within the cluster, followed by comparing its mean similarity to vegetation relevés within the nearest cluster. A silhouette width of 1 means that within-cluster similarity is much higher than between-cluster similarity, indicating the vegetation relevé is a good fit with the cluster. A value of −1 means that between-cluster similarity is much higher than within-cluster similarity, indicating the vegetation relevé is a poor fit with the cluster.

Appendix E. Supplementary data

Supplementary data associated with this article can be found in the online version, at https://doi.org/10.1016/j.rse.2019.01.018. These data include Google map of the most important areas described in this article.

References

Adam, E., Mutanga, O., Odindi, J., Abdel-Rahman, E.M., 2014. Land-use/cover classification in a heterogeneous coastal landscape using RapidEye imagery: evaluating the performance of random forest and support vector machines classifiers. Int. J. Remote Sens. 35, 3440–3458. https://doi.org/10.1080/01431161.2014.903435.

Berg, C., Abdank, A., Isermann, M., Jansen, F., Timmermann, T., Dengler, J., 2014. Red Lists and conservation prioritization of plant communities – a methodological framework. Appl. Veg. Sci. 17, 504–515. https://doi.org/10.1111/avsc.12093.

Betbeder, J., Rapinel, S., Corpetti, T., Pottier, E., Corgne, S., Hubert-Moy, L., 2014. Multitemporal classification of TerraSAR-X data for wetland vegetation mapping. J. Appl. Remote. Sens. 8, 083648. https://doi.org/10.1117/1.JRS.8.083648.

Betbeder, J., Rapinel, S., Corgne, S., Pottier, E., Hubert-Moy, L., 2015. TerraSAR-X dual-pol time-series for mapping of wetland vegetation. ISPRS J. Photogramm. Remote Sens. 107, 90–98. https://doi.org/10.1016/j.isprsjprs.2015.05.001. Multitemporal remote sensing data analysis.

Biondi, E., 2011. Phytosociology today: methodological and conceptual evolution. Plant Biosyst. Int. J. Deal. Asp. Plant Biol. 145, 19–29. https://doi.org/10.1080/11263504.2011.602748.

Biondi, E., Casavecchia, S., Pesaresi, S., 2011. Phytosociological synrelevés and plant landscape mapping: from theory to practice. Plant Biosyst. Int. J. Deal. Asp. Plant Biol. 145, 261–273.

Bonis, A., Bouzillé, J. aB, 2012. The project VegFrance: towards a national vegetation

database for France. Plant Sociol. 49, 97a99.
Bratsch, S.N., Epstein, H.E., Buchhorn, M., Walker, D.A., 2016. Differentiating among four Arctic tundra plant communities at Ivotuk, Alaska using field spectroscopy. Remote Sens. 8, 51. https://doi.org/10.3390/rs8010051.
Burai, P., Deák, B., Valkó, O., Tomor, T., 2015. Classification of herbaceous vegetation using airborne hyperspectral imagery. Remote Sens. 7, 2046–2066. https://doi.org/10.3390/rs70202046.
Cawley, G.C., Talbot, N.L., 2010. On over-fitting in model selection and subsequent selection bias in performance evaluation. J. Mach. Learn. Res. 11, 2079–2107.
Chasmer, L., Hopkinson, C., Veness, T., Quinton, W., Baltzer, J., 2014. A decision-tree classification for low-lying complex land cover types within the zone of discontinuous permafrost. Remote Sens. Environ. 143, 73–84. https://doi.org/10.1016/j.rse.2013.12.016.
Chen, B., Huang, B., Xu, B., 2015. Comparison of spatiotemporal fusion models: a review. Remote Sens. 7, 1798–1835.
Correll, M.D., Hantson, W., Hodgman, T.P., Cline, B.B., Elphick, C.S., Gregory Shriver, W., Tymkiw, E.L., Olsen, B.J., 2018. Fine-scale mapping of coastal plant communities in the northeastern USA. Wetlands. https://doi.org/10.1007/s13157-018-1028-3.
Davies, C.E., Moss, D., Hill, M.O., 2004. EUNIS habitat classification revised 2004. In: Rep. Eur. Environ. Agency-Eur. Top. Cent. Nat. Prot. Biodivers, pp. 127–143.
Davranche, A., Lefebvre, G., Poulin, B., 2010. Wetland monitoring using classification trees and SPOT-5 seasonal time series. Remote Sens. Environ. 114, 552–562. https://doi.org/10.1016/j.rse.2009.10.009.
De Cáceres, M., Chytrý, M., Agrillo, E., Attorre, F., Botta-Dukát, Z., Capelo, J., Czúcz, B., Dengler, J., Ewald, J., Faber-Langendoen, D., Feoli, E., Franklin, S.B., Gavilán, R., Gillet, F., Jansen, F., Jiménez-Alfaro, B., Krestov, P., Landucci, F., Lengyel, A., Loidi, J., Mucina, L., Peet, R.K., Roberts, D.W., Roleček, J., Schaminée, J.H.J., Schmidtlein, S., Theurillat, J.-P., Tichý, L., Walker, D.A., Wildi, O., Willner, W., Wiser, S.K., Scheiner, S., 2015. A comparative framework for broad-scale plot-based vegetation classification. Appl. Veg. Sci. 18, 543–560. https://doi.org/10.1111/avsc.12179.
Dengler, J., Bergmeier, E., Willner, W., Chytrý, M., 2013. Towards a consistent classification of European grasslands. Appl. Veg. Sci. 16, 518–520. https://doi.org/10.1111/avsc.12041.
Dumont, B., Rossignol, N., Loucougaray, G., Carrère, P., Chadoeuf, J., Fleurance, G., Bonis, A., Farruggia, A., Gaucherand, S., Ginane, C., Louault, F., Marion, B., Mesléard, F., Yavercovski, N., 2012. When does grazing generate stable vegetation patterns in temperate pastures? Agric. Ecosyst. Environ. 153, 50–56. https://doi.org/10.1016/j.agee.2012.03.003.
Duro, D.C., Franklin, S.E., Dubé, M.G., 2012. A comparison of pixel-based and object-based image analysis with selected machine learning algorithms for the classification of agricultural landscapes using SPOT-5 HRG imagery. Remote Sens. Environ. 118, 259–272. https://doi.org/10.1016/j.rse.2011.11.020.
Dusseux, P., Corpetti, T., Hubert-Moy, L., 2013. Temporal kernels for the identification of grassland management using time series of high spatial resolution satellite images. In: 2013 IEEE International Geoscience and Remote Sensing Symposium - IGARSS. Presented at the 2013 IEEE International Geoscience and Remote Sensing Symposium - IGARSS, pp. 3258–3260. https://doi.org/10.1109/IGARSS.2013.6723522.
Feilhauer, H., Schmidtlein, S., 2011. On variable relations between vegetation patterns and canopy reflectance. Ecol. Inform. 6, 83–92. https://doi.org/10.1016/j.ecoinf.2010.12.004.
Feilhauer, H., Thonfeld, F., Faude, U., He, K.S., Rocchini, D., Schmidtlein, S., 2013. Assessing floristic composition with multispectral sensors—a comparison based on monotemporal and multiseasonal field spectra. Int. J. Appl. Earth Obs. Geoinf. 21, 218–229. https://doi.org/10.1016/j.jag.2012.09.002.
Féret, J.B., Corbane, C., Alleaume, S., 2015. Detecting the phenology and discriminating Mediterranean natural habitats with multispectral sensors—an analysis based on multiseasonal field spectra. IEEE J. Sel. Top. Appl. Earth Obs. Remote Sens. 8, 2294–2305. https://doi.org/10.1109/JSTARS.2015.2431320.
Förster, M., Schmidt, T., Wolf, R., Kleinschmit, B., Fassnacht, F.E., Cabezas, J., Kattenborn, T., 2017. Detecting the spread of invasive species in central Chile with a Sentinel-2 time-series. In: 2017 9th International Workshop on the Analysis of Multitemporal Remote Sensing Images (MultiTemp). Presented at the 2017 9th International Workshop on the Analysis of Multitemporal Remote Sensing Images (MultiTemp), pp. 1–4. https://doi.org/10.1109/Multi-Temp.2017.8035216.
Franke, J., Keuck, V., Siegert, F., 2012. Assessment of grassland use intensity by remote sensing to support conservation schemes. J. Nat. Conserv. 20, 125–134. https://doi.org/10.1016/j.jnc.2012.02.001.
Gargominy, O., Tercerie, S., Daszkiewicz, P., Régnier, C., Ramage, T., Dupont, P., Poncet, L., 2012. TAXREF v5. 0, référentiel taxonomique pour la France: mise en œuvre et diffusion (Rapport SPN No. 32). SPN, Paris.
Guo, M., Li, J., Sheng, C., Xu, J., Wu, L., 2017. A review of wetland remote sensing. Sensors 17, 777. https://doi.org/10.3390/s17040777.
Hagolle, O., Huc, M., Villa Pascual, D., Dedieu, G., 2015. A multi-temporal and multi-spectral method to estimate aerosol optical thickness over land, for the atmospheric correction of FormoSat-2, LandSat, VENμS and Sentinel-2 images. Remote Sens. 7, 2668–2691. https://doi.org/10.3390/rs70302668.
Hauglin, M., Ørka, H.O., 2016. Discriminating between Native Norway Spruce and Invasive Sitka Spruce—a comparison of multitemporal Landsat 8 imagery, aerial images and airborne laser scanner data. Remote Sens. 8, 363. https://doi.org/10.3390/rs8050363.
Hennekens, S.M., Schaminée, J.H.J., 2001. TURBOVEG, a comprehensive data base management system for vegetation data. J. Veg. Sci. 12, 589–591. https://doi.org/10.2307/3237010.
Hijmans, R.J., 2015. raster: Geographic Data Analysis and Modeling.
Hill, M.O., 1979. TWINSPAN: A FORTRAN Program for Arranging Multivariate Data in an Ordered Two-way Table by Classification of Individual and Attributes. Cornell University Press.
Immitzer, M., Vuolo, F., Atzberger, C., 2016. First experience with Sentinel-2 data for crop and tree species classifications in Central Europe. Remote Sens. 8, 166. https://doi.org/10.3390/rs8030166.
Inglada, J., Vincent, A., Arias, M., Tardy, B., Morin, D., Rodes, I., 2017. Operational high resolution land cover map production at the country scale using satellite image time series. Remote Sens. 9, 95. https://doi.org/10.3390/rs9010095.
Jacob, A.L., Bonnell, T.R., Dowhaniuk, N., Hartter, J., 2014. Topographic and spectral data resolve land cover misclassification to distinguish and monitor wetlands in western Uganda. ISPRS J. Photogramm. Remote Sens. 94, 114–126. https://doi.org/10.1016/j.isprsjprs.2014.05.001.
Kaneko, K., Nohara, S., 2014. Review of effective vegetation mapping using the UAV (Unmanned Aerial Vehicle) method. J. Geogr. Inf. Syst. 6, 733.
Karasiak, N., Sheeren, D., Fauvel, M., Willm, J., Dejoux, J.F., Monteil, C., 2017. Mapping tree species of forests in southwest France using Sentinel-2 image time series. In: 2017 9th International Workshop on the Analysis of Multitemporal Remote Sensing Images (MultiTemp). Presented at the 2017 9th International Workshop on the Analysis of Multitemporal Remote Sensing Images (MultiTemp), pp. 1–4. https://doi.org/10.1109/Multi-Temp.2017.8035215.
Kaufman, L., Rousseeuw, P.J., 1990. Partitioning around medoids (program pam). In: Find. Groups Data Introd. Clust. Anal, pp. 68–125.
Khatami, R., Mountrakis, G., Stehman, S.V., 2016. A meta-analysis of remote sensing research on supervised pixel-based land-cover image classification processes: general guidelines for practitioners and future research. Remote Sens. Environ. 177, 89–100. https://doi.org/10.1016/j.rse.2016.02.028.
Kuhn, M., 2008. Caret package. J. Stat. Softw. 28, 1–26.
Kuhn, M., 2012. Variable Selection Using the Caret Package. (URL Httpcran Cermin Lipi Go Idwebpackagescaretvignettescaretselection Pdf).
Kuhn, M., Johnson, K., 2013. Applied Predictive Modeling. Springer.
Kumar, L., Sinha, P., 2014. Mapping salt-marsh land-cover vegetation using high-spatial and hyperspectral satellite data to assist wetland inventory. GIScience Remote Sens. 51, 483–497.
Landucci, F., Řezníčková, M., Šumberová, K., Chytrý, M., Aunina, L., Biță-Nicolae, C., Bobrov, A., Borsukevych, L., Brisse, H., Čarni, A., Csiky, J., Cvijanović, D., De Bie, E., De Ruffray, P., Dubyna, D., Dimopoulos, P., Dziuba, T., FitzPatrick, Ú., Font, X., Gigante, D., Golub, V., Hennekens, S.M., Hrivnák, R., Iemelianova, S., Jandt, U., Jenačković, D., Jansen, F., Kącki, Z., Lájer, K., Matulevičiutė, D., Mesterházy, A., Michalcová, D., Paal, J., Papastergiadou, E., Properzi, A., Radulović, S., Rodwell, J.S., Schaminée, J.H.J., Šilc, U., Sinkevičienė, Z., Stančić, Z., Stepanovich, J., Teteryuk, B., Tzonev, R., Venanzoni, R., Weekes, L., Willner, W., 2015. WetVegEurope: a database of aquatic and wetland vegetation of Europe. Phytocoenologia 45, 187–194. https://doi.org/10.1127/phyto/2015/0050.
Lausch, A., Bannehr, L., Beckmann, M., Boehm, C., Feilhauer, H., Hacker, J., Heurich, M., Jung, A., Klenke, R., Neumann, C., others, 2016. Linking Earth Observation and taxonomic, structural and functional biodiversity: local to ecosystem perspectives. Ecol. Indic. 70, 317–339.
Lavorel, S., Grigulis, K., Lamarque, P., Colace, M.-P., Garden, D., Girel, J., Pellet, G., Douzet, R., 2011. Using plant functional traits to understand the landscape distribution of multiple ecosystem services. J. Ecol. 99, 135–147. https://doi.org/10.1111/j.1365-2745.2010.01753.x.
Mahdavi, S., Salehi, B., Granger, J., Amani, M., Brisco, B., Huang, W., 2017. Remote sensing for wetland classification: a comprehensive review. GIScience Remote Sens. 0https://doi.org/10.1080/15481603.2017.1419602. (null).
Maltby, E., Acreman, M.C., 2011. Ecosystem services of wetlands: pathfinder for a new paradigm. Hydrol. Sci. J. 56, 1341–1359. https://doi.org/10.1080/02626667.2011.631014.
Maltby, E., Barker, T., 2009. The Wetlands Handbook. Wiley-Blackwell., Oxford.
Marion, B., Bonis, A., Bouzillé, J.-B., 2010. How much does grazing-induced heterogeneity impact plant diversity in wet grasslands? Ecoscience 17, 229–239. https://doi.org/10.2980/17-3-3315.
Martínez-López, J., Carreño, M.F., Palazón-Ferrando, J.A., Martínez-Fernández, J., Esteve, M.A., 2014. Remote sensing of plant communities as a tool for assessing the condition of semiarid Mediterranean saline wetlands in agricultural catchments. Int. J. Appl. Earth Obs. Geoinf. 26, 193–204. https://doi.org/10.1016/j.jag.2013.07.005.
Maxwell, A.E., Warner, T.A., Strager, M.P., Pal, M., 2014. Combining RapidEye Satellite Imagery and Lidar for Mapping of Mining and Mine Reclamation [WWW Document]. https://doi.org/info:doi/10.14358/PERS.80.2.179-189.
Maxwell, A.E., Warner, T.A., Fang, F., 2018. Implementation of machine-learning classification in remote sensing: an applied review. Int. J. Remote Sens. 39, 2784–2817. https://doi.org/10.1080/01431161.2018.1433343.
Mountrakis, G., Im, J., Ogole, C., 2011. Support vector machines in remote sensing: a review. ISPRS J. Photogramm. Remote Sens. 66, 247–259. https://doi.org/10.1016/j.isprsjprs.2010.11.001.
Mutanga, O., Adam, E., Cho, M.A., 2012. High density biomass estimation for wetland vegetation using WorldView-2 imagery and random forest regression algorithm. Int. J. Appl. Earth Obs. Geoinf. 18, 399–406. https://doi.org/10.1016/j.jag.2012.03.012.
Neumann, C., Weiss, G., Schmidtlein, S., Itzerott, S., Lausch, A., Doktor, D., Brell, M., 2015. Gradient-based assessment of habitat quality for spectral ecosystem monitoring. Remote Sens. 7, 2871–2898. https://doi.org/10.3390/rs70302871.
Ng, W.-T., Rima, P., Einzmann, K., Immitzer, M., Atzberger, C., Eckert, S., 2017. Assessing the potential of Sentinel-2 and Pléiades data for the detection of *Prosopis* and *Vachellia* spp. in Kenya. Remote Sens. 9, 74. https://doi.org/10.3390/rs9010074.
Oldeland, J., Dorigo, W., Lieckfeld, L., Lucieer, A., Jürgens, N., 2010. Combining vegetation indices, constrained ordination and fuzzy classification for mapping semi-natural vegetation units from hyperspectral imagery. Remote Sens. Environ. 114, 1155–1166. https://doi.org/10.1016/j.rse.2010.01.003.

Pereira, O.J.R., Melfi, A.J., Montes, C.R., 2017. Image fusion of Sentinel-2 and CBERS-4 satellites for mapping soil cover in the Wetlands of Pantanal. Int. J. Image Data Fusion 8, 148–172. https://doi.org/10.1080/19479832.2016.1261946.

R. Core Team, 2017. R: A Language and Environment for Statistical Computing. 2016 R Foundation for Statistical Computing, Vienna, Austria.

Rapinel, S., Clément, B., Magnanon, S., Sellin, V., Hubert-Moy, L., 2014. Identification and mapping of natural vegetation on a coastal site using a Worldview-2 satellite image. J. Environ. Manag. 144, 236–246. https://doi.org/10.1016/j.jenvman.2014.05.027.

Rapinel, S., Bouzillé, J.-B., Oszwald, J., Bonis, A., 2015a. Use of bi-seasonal Landsat-8 imagery for mapping marshland plant community combinations at the regional scale. Wetlands 1–12. https://doi.org/10.1007/s13157-015-0693-8.

Rapinel, S., Hubert-Moy, L., Clément, B., 2015b. Combined use of LiDAR data and multispectral earth observation imagery for wetland habitat mapping. Int. J. Appl. Earth Obs. Geoinf. 37, 56–64. https://doi.org/10.1016/j.jag.2014.09.002. (Special Issue on Earth observation for habitat mapping and biodiversity monitoring).

Rapinel, S., Rossignol, N., Gore, O., Jambon, O., Bouger, G., Mansons, J., Bonis, A., 2018. Daily monitoring of shallow and fine-grained water patterns in wet grasslands combining aerial LiDAR data and in situ piezometric measurements. Sustainability 10, 708. https://doi.org/10.3390/su10030708.

Refaeilzadeh, P., Tang, L., Liu, H., 2009. Cross-validation. In: Encyclopedia of Database Systems. Springer, pp. 532–538.

Robinson, T.P., Wardell-Johnson, G.W., Pracilio, G., Brown, C., Corner, R., van Klinken, R.D., 2016. Testing the discrimination and detection limits of WorldView-2 imagery on a challenging invasive plant target. Int. J. Appl. Earth Obs. Geoinf. 44, 23–30. https://doi.org/10.1016/j.jag.2015.07.004.

Rocchini, D., Foody, G.M., Nagendra, H., Ricotta, C., Anand, M., He, K.S., Amici, V., Kleinschmit, B., Förster, M., Schmidtlein, S., Feilhauer, H., Ghisla, A., Metz, M., Neteler, M., 2013. Uncertainty in ecosystem mapping by remote sensing. Comput. Geosci. 50, 128–135. https://doi.org/10.1016/j.cageo.2012.05.022.

Rodwell, J.S., Evans, D., Schaminée, J.H.J., 2018. Phytosociological relationships in European Union policy-related habitat classifications. Rend. Lincei Sci. Fis. E Nat. 1–13. https://doi.org/10.1007/s12210-018-0690-y.

Roelofsen, H.D., Kooistra, L., van Bodegom, P.M., Verrelst, J., Krol, J., Witte, J.-P.M., 2014. Mapping a priori defined plant associations using remotely sensed vegetation characteristics. Remote Sens. Environ. 140, 639–651. https://doi.org/10.1016/j.rse.2013.09.030.

Roth, K.L., Roberts, D.A., Dennison, P.E., Peterson, S.H., Alonzo, M., 2015. The impact of spatial resolution on the classification of plant species and functional types within imaging spectrometer data. Remote Sens. Environ. 171, 45–57. https://doi.org/10.1016/j.rse.2015.10.004.

Sanchez-Hernandez, C., Boyd, D.S., Foody, G.M., 2007. Mapping specific habitats from remotely sensed imagery: support vector machine and support vector data description based classification of coastal saltmarsh habitats. Ecol. Inform. 2, 83–88. https://doi.org/10.1016/j.ecoinf.2007.04.003.

Schmidt, T., Schuster, C., Kleinschmit, B., Förster, M., 2014. Evaluating an intra-annual time series for grassland classification—how many acquisitions and what seasonal origin are optimal? IEEE J. Sel. Top. Appl. Earth Obs. Remote Sens. 7, 3428–3439. https://doi.org/10.1109/JSTARS.2014.2347203.

Schmidtlein, S., Zimmermann, P., Schüpferling, R., Weiß, C., 2007. Mapping the floristic continuum: ordination space position estimated from imaging spectroscopy. J. Veg. Sci. 18, 131–140. https://doi.org/10.1111/j.1654-1103.2007.tb02523.x.

Schuster, C., Schmidt, T., Conrad, C., Kleinschmit, B., Förster, M., 2015. Grassland habitat mapping by intra-annual time series analysis – comparison of RapidEye and TerraSAR-X satellite data. Int. J. Appl. Earth Obs. Geoinf. 34, 25–34. https://doi.org/10.1016/j.jag.2014.06.004.

Shoko, C., Mutanga, O., 2017a. Examining the strength of the newly-launched Sentinel 2 MSI sensor in detecting and discriminating subtle differences between C3 and C4 grass species. ISPRS J. Photogramm. Remote Sens. 129, 32–40. https://doi.org/10.1016/j.isprsjprs.2017.04.016.

Shoko, C., Mutanga, O., 2017b. Seasonal discrimination of C3 and C4 grasses functional types: an evaluation of the prospects of varying spectral configurations of new generation sensors. Int. J. Appl. Earth Obs. Geoinf. 62, 47–55. https://doi.org/10.1016/j.jag.2017.05.015.

Tichý, L., 2002. JUICE, software for vegetation classification. J. Veg. Sci. 13, 451–453. https://doi.org/10.1111/j.1654-1103.2002.tb02069.x.

Tichý, L., Chytrý, M., Botta-Dukát, Z., 2014. Semi-supervised classification of vegetation: preserving the good old units and searching for new ones. J. Veg. Sci. 25, 1504–1512. https://doi.org/10.1111/jvs.12193.

Tomaselli, V., Adamo, M., Veronico, G., Sciandrello, S., Tarantino, C., Dimopoulos, P., Medagli, P., Nagendra, H., Blonda, P., 2016. Definition and application of expert knowledge on vegetation pattern, phenology, and seasonality for habitat mapping, as exemplified in a Mediterranean coastal site. Plant Biosyst. Int. J. Deal. Asp. Plant Biol. 0, 1–13. https://doi.org/10.1080/11263504.2016.1231143.

Ullerud, H.A., Bryn, A., Halvorsen, R., Hemsing, L.Ø., 2018. Consistency in land-cover mapping: influence of field workers, spatial scale and classification system. Appl. Veg. Sci. 21, 278–288.

Vanden Borre, J., Paelinckx, D., Mücher, C.A., Kooistra, L., Haest, B., De Blust, G., Schmidt, A.M., 2011. Integrating remote sensing in Natura 2000 habitat monitoring: prospects on the way forward. J. Nat. Conserv. 19, 116–125. https://doi.org/10.1016/j.jnc.2010.07.003.

Vrieling, A., Meroni, M., Darvishzadeh, R., Skidmore, A.K., Wang, T., Zurita-Milla, R., Oosterbeek, K., O'Connor, B., Paganini, M., 2018. Vegetation phenology from Sentinel-2 and field cameras for a Dutch barrier island. Remote Sens. Environ. 215, 517–529. https://doi.org/10.1016/j.rse.2018.03.014.

Wong, T.-T., 2015. Performance evaluation of classification algorithms by k-fold and leave-one-out cross validation. Pattern Recogn. 48, 2839–2846.

Yoshino, K., Kawaguchi, S., Kanda, F., Kushida, K., Tsai, F., 2014. Very high resolution plant community mapping at high moor, Kushiro wetland. Photogramm. Eng. Remote. Sens. 80, 895–905. https://doi.org/10.14358/PERS.80.9.895.

Zlinszky, A., Schroiff, A., Kania, A., Deák, B., Mücke, W., Vári, Á., Székely, B., Pfeifer, N., 2014. Categorizing grassland vegetation with full-waveform airborne laser scanning: a feasibility study for detecting Natura 2000 habitat types. Remote Sens. 6, 8056–8087. https://doi.org/10.3390/rs6098056.